Closecoupling studies of rotationally inelastic HF–HF collisions at hyperthermal energies

Millard H. Alexander

Citation: The Journal of Chemical Physics **73**, 5135 (1980); doi: 10.1063/1.439992
View online: http://dx.doi.org/10.1063/1.439992
View Table of Contents: http://scitation.aip.org/content/aip/journal/jcp/73/10?ver=pdfcov
Published by the AIP Publishing

Close-coupling studies of rotationally inelastic HF–HF collisions at hyperthermal energies

Millard H. Alexander

Department of Chemistry, University of Maryland, College Park, Maryland 20742
(Received 1 July 1980; accepted 25 July 1980)

Earlier close-coupling studies on the HF–HF system [A. E. DePristo and M. H. Alexander, J. Chem. Phys. **66**, 1334 (1977)] have been extended to larger channel bases, allowing the determination of converged integral cross sections for excitation out of the lower rotational levels of the bimolecular system. The calculations were confined to collision energies appropriate to supersonic beam experiments ($E = 0.5$–1.5 eV). Two potential surfaces were used, both taken from our earlier fit to *ab initio* points [M. H. Alexander and A. E. DePristo, J. Chem. Phys. **65**, 5009 (1976)]. In the first surface the symmetry of the only anisotropic term included corresponds to the standard dipole–dipole interaction; to which were added, in the second surface, a primarily repulsive anisotropy as well as the long-range dipole–quadrupole interaction. The largest cross sections (40–60 Å^2) are associated with R–R processes of the type $j_1 j_2 \rightarrow j_1 \pm 1, j_2 \mp 1$ which are dipole-allowed in first order. The magnitudes of these cross sections are little affected by the presence of the shorter-range anisotropic terms, since much of the inelasticity occurs at large impact parameter. Cross sections for processes which are dipole-allowed only in second or higher order are considerably smaller (1–10 Å^2), have classical dynamical thresholds at high energy, and are substantially lowered when the additional anisotropic terms are added to the potential, which has the effect of redirecting inelastic flux into the dipole forbidden channels. The cross sections for first order dipole–quadrupole transitions are also small, even in cases of near resonance. By contrast we find sizeable cross sections (7–15 Å^2) for transitions which are coupled only by the short range anisotropy, which implies that rotational energy transfer between polar molecules cannot be fully described by models which rely solely on the standard long-range multipole expansion of the potential.

I. INTRODUCTION

There has always been considerable interest, both theoretical as well as experimental, in the transfer of rotational energy between polar molecules.[1,2] Most likely this interest arises because the dipole–dipole interaction is well understood[3] compared with the more complex, shorter-range interactions which characterize nonpolar species. Recent experimental advances[4–11] now permit the study of rotationally inelastic polar molecule collisions with a greater degree of state resolution than has been hitherto possible. Hinchen[7] has used infrared–infrared double resonance to investigate the rotational relaxation of HF ($v = 1, j$) in collisions with HF. By monitoring collision-induced changes in the infrared emission of a hot HCl beam, Ding and Polanyi[5] have studied the relaxation of HCl ($v = 1, j$) with HCl and HF targets. Crim and co-workers[11] have used dye laser excitation and time resolved visible fluorescence detection to probe rotational self-relaxation in the $v = 3$, 4 levels of HF. Recently, with laser-induced fluorescence detection, Dagdigian and Wilcomb[8,9] measured integral cross sections for the rotationally inelastic scattering of supersonic beams of LiH ($v = 0$, $j = 1$) in collisions with HCl, DCl, and HCN.

This experimental work poses new tests of our ability to model the collision dynamics. In the past, most theoretical work was based on the perturbative (Born) solution of the time dependent classical path equations.[3,12–14] By comparison with more exact theoretical calculations,[15] as well as with the experimental results from Dagdigian's laboratory,[8,9] we have shown that the Born approximation (BA) tends to overestimate considerably the cross sections for dipole allowed transitions. The failure of the BA becomes more pronounced, at least for the systems we have studied,[9,16] in the case of transitions which are dipole allowed only in second or higher order. Unfortunately, as we have demonstrated,[8,9,16,17] even at hyperthermal velocities application of the sudden approximation[14,18,19] is not fully justified, due to the extreme range of the dipole–dipole potential. We have recently developed[16,17] a simple adiabatic correction to the sudden approximation which yields cross sections in good agreement with the experimental values obtained by Dagdigian for the LiH + HCl, DCl, and HCN systems. Similarly, the experimental findings of Ding and Polanyi[5] have been reproduced reasonably well by the classical trajectory studies of Polanyi and Sathyamurthy,[20] as well as Turfa and Marcus.[21]

Unfortunately, the fundamental fully resolved cross sections are not accessible even in the most sophisticated experiments. Thus, experimental data alone do not provide a full test of the accuracy and physical correctness of a dynamical approximation. It is therefore important to determine theoretically, for a prototype system, a set of exact cross sections which can then be used to provide the necessary feedback in the development of accurate approximation techniques.

The HF–HF system is an appropriate prototype for rotationally inelastic collisions between polar molecules. There have been several full *ab initio* surfaces determined for this system,[22–24] one of which we have fitted[25] to an analytic representation suitable for quantum scattering calculations.[26] The wide rotational spacing of the HF molecule suggests that converged cross sections might be obtained with channel bases of manageable size. Several years ago we published[15] the results of some exploratory quantum close-coupling calculations on the HF–HF system. Subsequently, Alper, Carrol, and Gelb[27] reported equivalent calculations using the quasi-

 0021-9606/80/225135-12$01.00

classical trajectory treatment of the dynamics. Although the scope of our quantum study was initially limited by the computer hardware available, over the past year we have been able to carry out far more extensive calculations using the facilities of the National Resource for Computation in Chemistry.

The present article reports the results of these new calculations. We have used two interaction potentials taken from our earlier fit[25]: a simplified surface consisting of a dipole–dipole anisotropy and a repulsive spherically symmetric term, and a more complete surface obtained by adding dipole–quadrupole and shorter range anisotropic terms. These surfaces are described in the next section. The comparison between the cross sections corresponding to the simplified and full surfaces can shed light on the relative role of the dipole–dipole and shorter-range forces, which has been the subject of speculation.[8] The technical details of the scattering calculations are given in Sec. III. We restricted the present study to collisions at hyperthermal velocities ($v_{rel}=3-6\times10^5$ cm/s), as would occur in molecular beam experiments involving supersonic sources.[4,6,8-10] The resulting integral cross sections are presented and analyzed in Secs. IV and V. A brief discussion follows.

II. POTENTIAL SURFACES

The two HF molecules are treated as rigid rotors. In a space-fixed (SF) frame the scalar interaction potential is expanded as a sum of products of spherical harmonics, namely[28]

$$V(\hat{r}_1, \hat{r}_2, \mathbf{R}) = \sum_{\lambda_1\lambda_2\lambda} A_{\lambda_1\lambda_2\lambda}(R)\, Y_{\lambda_1\lambda_2\lambda}(\hat{r}_1, \hat{r}_2, \hat{R}) , \qquad (1)$$

where $\hat{r}_1$ and $\hat{r}_2$ denote the orientations of the two molecular axes, $\mathbf{R}$ is the vector separation between the centers-of-mass of the two molecules, and the quantity $Y_{\lambda_1\lambda_2\lambda}$ is a scalar product of spherical harmonics, namely

$$Y_{\lambda_1\lambda_2\lambda} = \sum_{m_1 m_2 m} (\lambda_1 m_1 \lambda_2 m_2 | \lambda m)\, Y_{\lambda_1 m_1}(\hat{r}_1)\, Y_{\lambda_2 m_2}(\hat{r}_2)\, Y^*_{\lambda m}(\hat{R}) . \qquad (2)$$

where $(\cdots\cdots|\cdots)$ is a Clebsch–Gordan coefficient. The sum $\lambda_1+\lambda_2+\lambda$ must be even to ensure invariance under inversion of the SF coordinate system. Additionally, in the present case of identical molecules, interchange symmetry implies that[29]

$$A_{\lambda_2\lambda_1\lambda} = (-1)^{\lambda_1+\lambda_2} A_{\lambda_1\lambda_2\lambda} . \qquad (3)$$

As discussed in the Introduction, two potential surfaces were used in the present paper. The first or simplified surface contains two terms, the first of these being a spherically symmetric interaction, A_{000},

$$A_{000}(R) = 1.324\times10^5 e^{-2R} - 977.1\, e^{-1.1R} , \qquad (4)$$

with energy in eV and distance in bohrs. This basically repulsive potential has a hard sphere radius of 5.46 bohr and a small well 0.012 eV deep at $R=6.12$ bohr.[30] The second component in the simplified surface, A_{112}, has the symmetry of the long-range dipole–dipole interaction and is given by the expression

$$A_{112}(R) = -21.28\, e^{-R} - 1.954\, e^{-0.475R} - 227.2R^{-3} . \qquad (5)$$

The third term in Eq. (5), which contains the asymptotic dependence, corresponds to the interaction of two dipoles of magnitude 1.82 D, the experimental value for the HF molecule. Even at $R=5.46$ bohr, the hard sphere radius of the spherically symmetric potential, the two exponential terms in Eq. (5) contribute together only 14% of the magnitude of the anisotropic term. Since the only anisotropy included has dipole–dipole symmetry, the most attractive configuration on the simplified surface is a collinear alignment with both molecules pointing in the same direction. The minimum in this geometry occurs at a center-of-mass separation of 5.07 bohr with a well depth of −0.22 eV. This compares reasonably well with the experimental separation[31] ($R=5.27$ bohr) and dissociation energy[32] ($D_e=0.26\pm0.07$ eV) of the $(HF)_2$ dimer, although the experimental geometry is somewhat bent from colinearity.

In addition, we also used what will be denoted as a "full" surface, which consists of the simplified surface discussed in the preceding paragraph with two additional anisotropic terms. The first of these, A_{123}, and its symmetric partner, A_{213}, have the symmetry of the long-range dipole–quadrupole and quadrupole–dipole interactions. The functional dependence on R is given by

$$A_{123}(R) = -A_{213}(R) = -(1.824\cdot10^4/R - 4343)\, e^{-2.04R} + 634.9/R^4 . \qquad (6)$$

The asymptotic behavior, contained in the last term, corresponds to the interaction of a dipole of magnitude 1.82 D and a quadrupole of magnitude 2.6 D·Å, both of these being the experimental values for the HF molecule. As in the case of the dipole–dipole term [Eq. (5)], the deviation from the asymptotic behavior is small; at $R=5.5$ bohr the exponential terms in Eq. (6) contribute only 2% of the total magnitude.

The second term included in the full surface, A_{011} (and A_{101}) is the largest of the short-ranged anisotropic components in our fit[25] to the *ab initio* surface of Yarkony *et al.*[22] Explicitly, we have

$$A_{011}(R) = -A_{101}(R) = -7947\, e^{-1.9R} + 26.49\, e^{-0.7885R} . \qquad (7)$$

As discussed in our earlier paper[25] the minimum in the full surface occurs at $R=5.5$ bohr with a well depth of 0.29 eV and a slightly bent geometry. The functional dependence on R of the A_{000}, A_{011}, A_{112}, and A_{123} terms is illustrated in Fig. 2 of Ref. 25.

Both the simplified and full surfaces contain a fairly reasonable description of the bond strength and geometry of the $(HF)_2$ dimer.[33] Thus we can expect that the effect of the strong so-called "hydrogen bonding" forces on rotational energy transfer will be adequately revealed in the subsequent scattering calculations.

III. SCATTERING CALCULATIONS

The collision dynamics were treated by full close-coupling in a space-fixed frame.[15,29,34] The total wave function is expanded as a sum of products of the rotational wave functions of the colliding molecules. This leads to a set of coupled ordinary differential equations

which must be solved numerically. Each channel is indexed by the molecular rotational angular momenta of the two molecules, j_1 and j_2; by the magnitude of the vector resultant j_{12}; by the orbital angular momentum l; and by the total angular momentum J, where

$$\mathbf{J} = \mathbf{j}_{12} + \mathbf{l} = \mathbf{j}_1 + \mathbf{j}_2 + \mathbf{l} \ . \tag{8}$$

For given values of J, j_1, and j_2 the number of allowable values of j_{12} and l, and consequently the number of coupled equations, can be large, even for small values of j_1 and j_2. This proliferation is alleviated somewhat by the fact that there is no coupling between channels corresponding to different total parity, $(-1)^{j_1+j_2+l}$. Additionally, in the present case of the scattering of identical molecules, interchange symmetry allows a further decoupling of the equations.[15,29,35] The net consequence is that for each value of the total angular momentum J, there exist four distinct sets of coupled differential equations corresponding to positive (+) and negative (−) interchange symmetry and even and odd total parity. These sets are of unequal dimension and alternate with J as follows[15]: The even parity (+) set at even J is equivalent to the odd parity (−) set at odd J; similarly the even parity (−) set at even J becomes the odd parity (+) set at odd J. An equivalent reversal applies to the even parity sets at odd J. It should be noted that only one channel is associated with the $j_1 j_2 = 00$ state, and that this channel occurs in the (+) symmetry, even parity set at even J and in the (−) symmetry, odd parity set at odd J.

Explicit expressions for the potential matrix elements have been given before.[15,29,34] A given $\lambda_1\lambda_2$ term in the expansion (1) will couple the rotational states $j_1 j_2$ and $j_1' j_2'$ only if the triangular inequalities,

$$|j_1 - j_1'| \le \lambda_1 \le j_1 + j_1' \tag{9}$$

and

$$|j_2 - j_2'| \le \lambda_2 \le j_2 + j_2' \ , \tag{10}$$

are satisfied, and only if the following parity conditions are met:

$$(-1)^{j_1+j_1'+\lambda_1} = (-1)^{j_2+j_2'+\lambda_2} = 1 \ . \tag{11}$$

This latter implies[15] that in the case of the simplified potential, where $\lambda_1 = \lambda_2 = 1$, there will be no coupling between states of differing rotational parity, defined as $(-1)^{j_1+j_2}$. This results in a further block diagonalization of the coupled equations.

These equations are propagated numerically into the asymptotic region. An S matrix is then extracted in the usual manner.[36] The degeneracy averaged integral cross section for the inelastic $j_1 j_2 \to j_1' j_2'$ transition is given as a sum over the total angular momentum, J, namely,

$$\sigma^{\pm}_{j_1 j_2 \to j_1' j_2'} = \pi k^{-2}_{j_1 j_2} \sum_J P^{J\pm}_{j_1 j_2 \to j_1' j_2'} \ , \tag{12}$$

where the partial opacity, $P^{J\pm}_{j_1 j_2 \to j_1' j_2'}$, is defined by

$$P^{J\pm}_{j_1 j_2 \to j_1' j_2'} = \frac{[J]}{[j_1][j_2]} \sum_{\substack{l,l' \\ j_{12}, j_{12}'}} |S^{J\pm}_{j_1 j_2 j_{12} l, j_1' j_2' j_{12}' l'}|^2 \ , \tag{13}$$

and the summation extends over both total parities but is restricted to S-matrix elements of either (+) or (−) interchange symmetry. The wave vector in Eq. (12) is defined by

$$k^2_{j_1 j_2} = 2\mu(E - \epsilon_{j_1 j_2})/\hbar^2 \ , \tag{14}$$

where μ is the collision reduced mass, and $\epsilon_{j_1 j_2}$ denotes the internal rotational energy of the bimolecular system. Table I lists the values of these internal energies for the lowest channels. We have mentioned above that there exists only one channel containing the $j_1 j_2 = 00$ level, which corresponds to (+) symmetry at even J and (−) symmetry at odd J. Consequently, for transitions involving the $j_1 j_2 = 00$ level, the summation in Eq. (12) is restricted to even or odd J-values.

TABLE I. HF–HF channel energies.[a]

j_1	j_2	$\epsilon_{j_1 j_2}$ (cm^{-1})
0	0	0.0
0	1	41.1
1	1	82.2
0	2	123.3
1	2	164.4
2	2	246.6
0	3	246.4
1	3	287.5
2	3	369.7
3	3	492.8
0	4	410.3
1	4	451.4
2	4	533.6
3	4	656.8
0	5	614.9
1	5	656.0

[a]Energies determined using the experimental values of the HF ($v = 0$) rotational constants, $B_0 = 20.5596$ cm^{-1} and $D_0 = 0.002117$ cm^{-1} [D. U. Webb and K. N. Rao, J. Mol. Spectrosc. **28**, 121 (1968)].

As discussed by Zarur and Rabitz,[28] the physical cross section is a linear combination of σ^+ and σ^-, namely,

$$\sigma_{j_1 j_2 \to j_1' j_2'} = W^+ \sigma^+_{j_1 j_2 \to j_1' j_2'} + W^- \sigma^-_{j_1 j_2 \to j_1' j_2'} \ , \tag{15}$$

where W^+ and W^- are fractional weights which reflect the nuclear spin statistics and which sum to unity. Since the sets of coupled equations of (+) symmetry at even values of J are equivalent to the sets of (−) symmetry at odd values of J and vice versa, to a good approximation

$$\frac{1}{[J]} P^{J\pm}_{j_1 j_2 \to j_1' j_2'} \simeq \frac{1}{[J+1]} P^{(J+1)\mp}_{j_1 j_2 \to j_1' j_2'} \ . \tag{16}$$

Any slight differences will average out at moderate to high collision energies, where typically 500–1200 values of J must be included. At these energies the (+) and (−) cross sections are virtually identical. Thus we can relate the physical cross section to an interchange averaged opacity, in other words,

$$\sigma_{j_1 j_2 \to j_1' j_2'} = \pi k^{-2}_{j_1 j_2} \sum_J P^J_{j_1 j_2 \to j_1' j_2'} \ , \tag{17}$$

where

$$P^{J}_{j_1 j_2 - j_1' j_2'} = \tfrac{1}{2}(P^{J+}_{j_1 j_2 - j_1' j_2'} + P^{J-}_{j_1 j_2 - j_1' j_2'}) \ . \quad (18)$$

In the present study, for the simplified (dipole–dipole) potential surface we have obtained S matrices and integral cross sections at nine total energies ranging from 3900 cm^{-1} (0.4835 eV) to 12500 cm^{-1} (1.5498 eV). These correspond to relative translational velocities of 3×10^5 cm/s to 6×10^5 cm/s, as would occur in supersonic beam experiments.[4,6,8,9] These energies are sufficiently high compared with the $(HF)_2$ well depth, that it is unlikely that shape resonance effects (orbiting collisions) would contribute significantly. The coupled equations were solved using a modified version[37] of Gordon's code.[36,38] Although a recent workshop sponsored by the National Resource for Computation in Chemistry (NRCC) has concluded[39] that other codes may now be superior for many types of collision problem, the Gordon code is ideally suited to the present application involving long-range forces and short deBroglie wavelengths. The deBroglie wave lengths for all channels ranged from ~0.02 bohr at E = 12500 cm^{-1} to ~0.03 bohr at E = 3900 cm^{-1}, which is much smaller than the range of the potential (~15 bohr). Typically only 20–25 integration steps were required to propagate the CC equations into the asymptotic region.

The modified Gordon code[37] (QCOL/MK2) was developed initially at the University of Maryland and then transferred to the NRCC for further software changes and subsequent production runs on the CDC 7600 at the Lawrence Berkeley Laboratory (LBL). All the calculations at LBL were set up and executed remotely, using the TYMNET dial-up network. The output from each run was structured so that the partial opacities and other key parameters could be extracted interactively, with the complete output then being written on microfiche. The whole procedure was very convenient. We were able to take real advantage of the 3 h difference between Eastern and Pacific Standard Time by carrying out the bulk of our interactive work during EST morning hours, when demand use at LBL was negligible.

The input tolerance parameters and integration step sizes were chosen, after some initial experimentation, to ensure that the resulting partial opacities [Eq. (12)] were sufficiently accurate for the computation of the large cross sections of interest here. With the Gordon algorithm calculations at the initial collision energy are considerably more time consuming than at subsequent energies, where the previously computed transformation matrices can be utilized unchanged.[36] Unfortunately, loss in accuracy occurs unless the subsequent energies lie fairly close to the initial value. In the present work initial energy calculations were performed at E = 12 500, 8000, and 5300 cm^{-1}. For each value of the total energy partial opacities for all parity and interchange sets were determined at ~50 values of J. Linear interpolation was then used to calculate the corresponding integral cross sections.

The channel bases used are summarized in Table II. Due to the many j_{12} and l values which must be included for the higher $j_1 j_2$ pairs, the number of channels rapidly becomes very large, despite the reductions allowed by parity and interchange symmetry. For the simplified potential the bases, which include only states of even rotational parity, $(-1)^{j_1+j_2}$, correspond to successively higher orders of dipole–dipole coupling from the $j_1 j_2$ = 00 level. The channel bases are identical to those defined in our previous study,[15] except that the $j_1 j_2$ = 44 channels have been eliminated from the B5 basis. Including these raises the dimensionality of the largest parity-interchange set to 96 channels. The storage requirements for this large a calculation would have exceeded the small core memory of the CDC 7600 and thereby necessitated significant modifications, which were not made.

For the full surface the dimensionality problem becomes even more acute, since coupling now occurs between states of differing rotational parity, $(-1)^{j_1+j_2}$. The channel bases were expanded to include some of the intermediate levels of odd rotational parity which were excluded in the case of B3 and B4 bases for the simplified surface. The restrictions on dimensionality discussed in the preceding paragraph precluded addition of the $j_1 j_2$ = 04, 14, and 24 levels. Because of these limitations the calculations with the full surface were performed at only the six highest energies (E = 6000 – 12 500 cm^{-1}), where, as will be seen in the next section, the

TABLE II. Summary of scattering calculations: channel bases and computation times.

Basis[a]	Rotor states ($j_1 j_2$)	Channels[b]	Time (s)[c] 1st	2nd
		Dipole–dipole potential		
B3	00, 11, 02, 22	17+10+10+8	3.4	0.6
B4	00, 11, 02, 22, 13, 33	44+32+32+28	38	4.4
B5	00, 11, 02, 22, 13, 33, 04, 24	72+58+58+56	79	19
		Full potential		
B3	00, 01, 11, 02, 12, 22, 03	31+22+21+21	23	2.4
B4	00, 01, 11, 02, 12, 22, 03, 13, 23, 33	76+60+60+60	140[d]	27

[a]For the dipole–dipole potential the channel bases are identical to those used in Ref. 15, except that here the $j_1 j_2$ = 44 channels have not been included in the B5 levels.

[b]Total number of channels. The four entries correspond, for even values of J, to the interchange symmetry and parity sets (+) even, (–) odd, (+) odd, and (–) even, respectively.

[c]CPU time requirement on CDC-7600 for determination of a complete S matrix (all parity and interchange sets) for one value of J. The two entries refer to the time requirements of an "initial energy" calculation, involving the computation of the local transformation matrices (Refs. 36, 37), and to the time requirements of a "subsequent energy" calculations where the previously determined transformation matrices are used.

[d]In comparison to the B5 calculations with the dipole–dipole potential, the increased time here reflects primarily the calculation of the additional angular momentum coefficients (Ref. 15) required by the A_{011} and A_{123} terms in the potential.

TABLE III. Classification scheme for rotationally inelastic transitions.

Type	Transitions
Dipole–dipole $T \rightarrow R$	
First order	$00 \rightarrow 11$, $11 \rightarrow 22$, $01 \rightarrow 12$
Second order	$00 \rightarrow 02$, $00 \rightarrow 22$, $11 \rightarrow 13$
Third order	$00 \rightarrow 13$
Dipole–dipole $R \rightarrow R$	$11 \rightarrow 02$, $22 \rightarrow 13$, $12 \rightarrow 03$
Dipole–quadrupole $T \rightarrow R$	$00 \rightarrow 12$
Dipole–quadrupole $R \rightarrow R$	$11 \rightarrow 03$, $22 \rightarrow 03$
Short-range $T \rightarrow R$	$00 \rightarrow 01$, $01 \rightarrow 11$, $11 \rightarrow 12$, $12 \rightarrow 22$, $03 \rightarrow 13$

B4 basis cross sections are expected to be reasonably well converged. Typical computer times are shown in Table II; the numbers correspond to the total time for all four parity and interchange sets at a single value of J and refer to the CDC 7600 at LBL. The time savings for the subsequent energy calculations are evident.

IV. RESULTS: DIPOLE–DIPOLE POTENTIAL

We examine first the results for the simplified potential. In the discussion of the computed cross sections and partial opacities it will be useful to separate the various transitions into $T \rightarrow R$ and $R \rightarrow R$ processes and to identify the leading terms in the potential which couple the particular initial and final states. This classification scheme is presented in Table III. For consistency with our previous study,[15] all the cross sections and opacities are labeled so that the final state is energetically higher than the initial state. The corresponding quantities for the reverse transition can be obtained from the standard microreversibility relation

$$\sigma_{j_1' j_2' \rightarrow j_1 j_2} = \frac{[j_1][j_2]k^2_{j_1 j_2}}{[j_1'][j_2']k^2_{j_1' j_2'}} \sigma_{j_1 j_2 \rightarrow j_1' j_2'} , \tag{19}$$

and similarly for the partial opacities. In the usual quantum formulation of the collision between identical molecules, the two molecules must be treated as indistinguishable.[28,29,35] Thus, it is not possible to observe the perfectly resonant R–R transitions of the type $j_1 j_2 \rightarrow j_2 j_1$. In principle, one can define an S matrix for the interchange of quantum numbers in terms of the properly antisymmetrized elastic S matrices, namely[40,41]

$$\tilde{S}^J_{j_1 j_2 j_{12} l, j_2 j_1 j_{12} l} = \tfrac{1}{2}(S^{J-}_{j_1 j_2 j_{12} l, j_1 j_2 j_{12} l} - S^{J+}_{j_1 j_2 j_{12} l, j_1 j_2 j_{12} l}) , \tag{20}$$

where the superscript tilde denotes the nonsymmetrized quantity. We did not, however, compute any $j_1 j_2 \rightarrow j_2 j_1$ cross sections,[41] since these are not observables.

Integral cross sections for the $00 \rightarrow 11$, 02, 22, 12; $11 \rightarrow 02$, 22, 13; and $22 \rightarrow 13$ transitions are listed in Table IV. Values are given for each of the channel

TABLE IV. Integral cross sections (Å^2); dipole–dipole potential.[a]

		Total energy (cm^{-1})								
Transition	Basis[a]	3900	4600	5300	6000	7000	8000	9500	11 000	12 500
$00 \rightarrow 11$	$B3$	28.4	36.4	43.1	48.4	55.0	60.6	65.8	68.4	69.7
	$B4$	36.9	41.9	47.0	50.3	54.1	56.7	58.4	58.7	57.7
	B5	33.4	39.7	46.8	48.0	54.0	57.2	61.0	60.5	57.6
$00 \rightarrow 02$	B3	1.7	2.2	2.9	3.6	4.6	5.5	6.6	7.5	8.1
	B4	3.0	3.9	4.6	5.5	6.7	7.7	8.6	9.1	9.2
	B5	2.5	2.8	4.1	6.9	8.5	9.6	10.0	9.8	9.3
$00 \rightarrow 22$	B3	0.1	0.2	0.4	0.6	1.1	1.9	3.5	5.5	7.6
	B4	0.5	1.0	1.6	2.6	4.4	6.6	10.0	13.5	16.6
	B5	1.9	2.3	3.1	4.4	6.6	11.3	12.4	15.1	16.5
$00 \rightarrow 13$	B3[b]	...	...	...	...	...	...	...	...	...
	B4	0.1	0.1	0.2	0.5	0.9	1.4	2.3	3.3	4.4
	B5	0.4	0.4	0.6	1.2	2.1	3.3	5.1	7.5	8.9
$11 \rightarrow 02$	B3	43.1	48.3	52.4	55.6	57.4	58.4	57.6	56.4	54.8
	B4	49.5	54.5	57.6	59.1	59.4	58.5	55.9	53.1	50.4
	B5	48.9	54.0	56.1	57.4	56.7	55.6	53.1	50.7	47.7
$11 \rightarrow 22$	B3	2.9	3.7	4.6	5.4	6.6	8.0	9.2	10.6	12.0
	B4	5.2	6.1	7.0	7.8	8.9	10.0	11.3	12.5	13.6
	B5	7.6	8.6	9.0	9.8	10.8	11.6	12.7	13.5	13.7
$11 \rightarrow 13$	B3[b]	...	...	...	...	...	...	...	...	...
	B4	1.0	1.5	2.1	2.7	3.7	4.8	6.4	8.0	9.5
	B5	2.0	2.8	3.5	5.3	7.1	8.5	10.5	12.4	13.5
$22 \rightarrow 13$	B3[b]	...	...	...	...	...	...	...	...	...
	B4	55.7	62.0	66.1	68.6	70.2	70.9	69.8	68.1	66.1
	B5	61.8	68.8	70.3	68.5	68.6	68.2	64.4	61.7	58.7

[a]See Table II for description of channel bases.

[b]These transitions are not allowed with a B3 basis.

TABLE V. Integral $j_1 j_2 \rightarrow j_1' j_2'$ cross sections (Å^2), dipole–dipole potential, B5 channel basis.

	$j_1 j_2 = 11$				$j_1 j_2 = 22$		
E (cm^{-1})	$j_1' j_2' = 02$[a]	00[b]	22[a]	13[a]	00[b]	11[b]	13[a]
3900	48.9	3.8	7.6	2.0	0.08	2.9	61.8
4600	54.0	4.5	8.6	2.8	0.10	3.2	68.8
5300	56.1	5.3	9.0	3.5	0.13	3.3	70.3
6000	57.4	5.4	9.8	5.3	0.18	3.6	68.5
7000	56.7	6.1	10.8	7.1	0.27	4.0	68.6
8000	55.6	6.4	11.6	8.5	0.47	4.3	68.2
9500	53.1	6.8	12.7	10.5	0.51	4.7	64.4
11000	50.7	6.8	13.5	12.4	0.62	4.9	61.7
12500	47.7	6.4	13.7	13.5	0.67	5.0	58.7

[a]Values taken from Table IV.
[b]Values derived from entries in Table IV using microscopic reversibility.

bases described in Table II. In consideration of the tolerance parameters used in the present calculations, we estimate that the probable accuracy of the cross sections is ± 1.0 Å^2. Cross sections for upward transitions from the $j_1 j_2 = 22$ (except for 22 → 13), 13, 33, or 04 levels were not determined, since it is unlikely that the values would be converged with the basis sets used. Representative partial opacities are displayed in Fig. 1 for total energies of 12500 cm^{-1} and 5300 cm^{-1}. The opacities are plotted against the total angular momentum and against the corresponding semiclassical impact parameter, defined by

$$b = J/k_{j_1 j_2} . \tag{21}$$

It is clear that the cross sections for all the transitions considered, with the possible exception of 00 → 13, are converged with respect to channel basis at the higher energies. At the lower energies only the cross sections for the first-order dipole coupled 00 → 11 and 11 → 02 transitions are demonstrably converged, although we estimate that the 00 → 02, 22 → 13, and 11 → 22 cross sections are likely converged to within the accuracy of the calculations. It seems reasonable that convergence is more rapid at higher energies where the coupling due to the slowly varying dipole–dipole potential becomes relatively weaker. Eventually, at still higher energies, the perturbative two-state limit will be reached.

Examination of the partial opacity plots reveals a bimodal distribution for nearly all the transitions. A similar bimodal structure is apparent in the opacity plots reported by Alper *et al.*[27] in their classical trajectory studies of the 00 → 11, 02, and 22 transitions at $E = 8000$ cm^{-1}. The dip in the partial opacity curves implies that over a narrow range of impact parameters the effective torque exerted on the collision partners is substantially reduced. Possibly this reflects an interplay between the spherically symmetric repulsion and the purely attractive anisotropy. In any case, the partial opacity curves reveal that the major contributions to the inelastic cross sections result from collisions at impact parameters considerably beyond the minimum in the potential well ($R \approx 5.5$ bohr). This is especially true for the first-order dipole-allowed processes (00 → 11, 11 → 02, 22 → 13). Thus, at least at the collision energies under consideration here, complex formation due to "hydrogen bonding" forces does not appear to play a major role in rotational relaxation or transfer.

We turn now to an examination of the energy dependence of the cross sections. As with most inelastic processes we expect the cross sections to rise steeply with increasing energy, reach a maximum, which corresponds to the classical dynamical threshold[42] for the transition, and then fall slowly as the energy increases further. It is clear that the entire energy range spanned here encompasses the maxima in the first-order R–R (11 → 02, 22 → 13), first-order T–R (00 → 11, 11 → 22) transitions, and the second-order 00 → 02, T–R transition. For the other second- and third-order T–R processes (00 → 22, 13; 11 → 13) the cross sections rise monotonically over the energy range spanned here. It is interesting that the classical dynamical thresholds for the latter transitions occur at such high energy. Also, for a given transition the convergence with channel basis appears to become more rapid at energies beyond the dynamical threshold.

We have shown in another publication[43] that the cross sections presented here can not be fit well by any of the recent energy gap parametrization models.[44–46] In fact, the role played by the initial and final rotational quantum numbers is better understood in a group-theoretic rather than statistical framework.[41,47,48] We refer the interested reader to the mentioned article[43] for more details.

Recently DePristo and Rabitz[41] have applied their energy corrected sudden scaling relations[49] to the collision of two diatomic molecules and, in particular, to the HF–HF system. In their analysis[41] they conclude that the T–R and R–R transitions must be treated separately since the effective range of the potential is so much greater for the latter processes. This implies, of course, that for a given initial state, the R–R cross sections will be much larger than the various R–T (or T–R) cross sections. For the present system this can be seen clearly in Table V, where we compare B5 R–R and R–T cross sections for transitions out of the $j_1 j_2 = 11$ and 22 levels. For the purpose of this comparison some of the cross sections for upward transitions from Table IV have been converted to values for the comparable downward transition by means of micro-

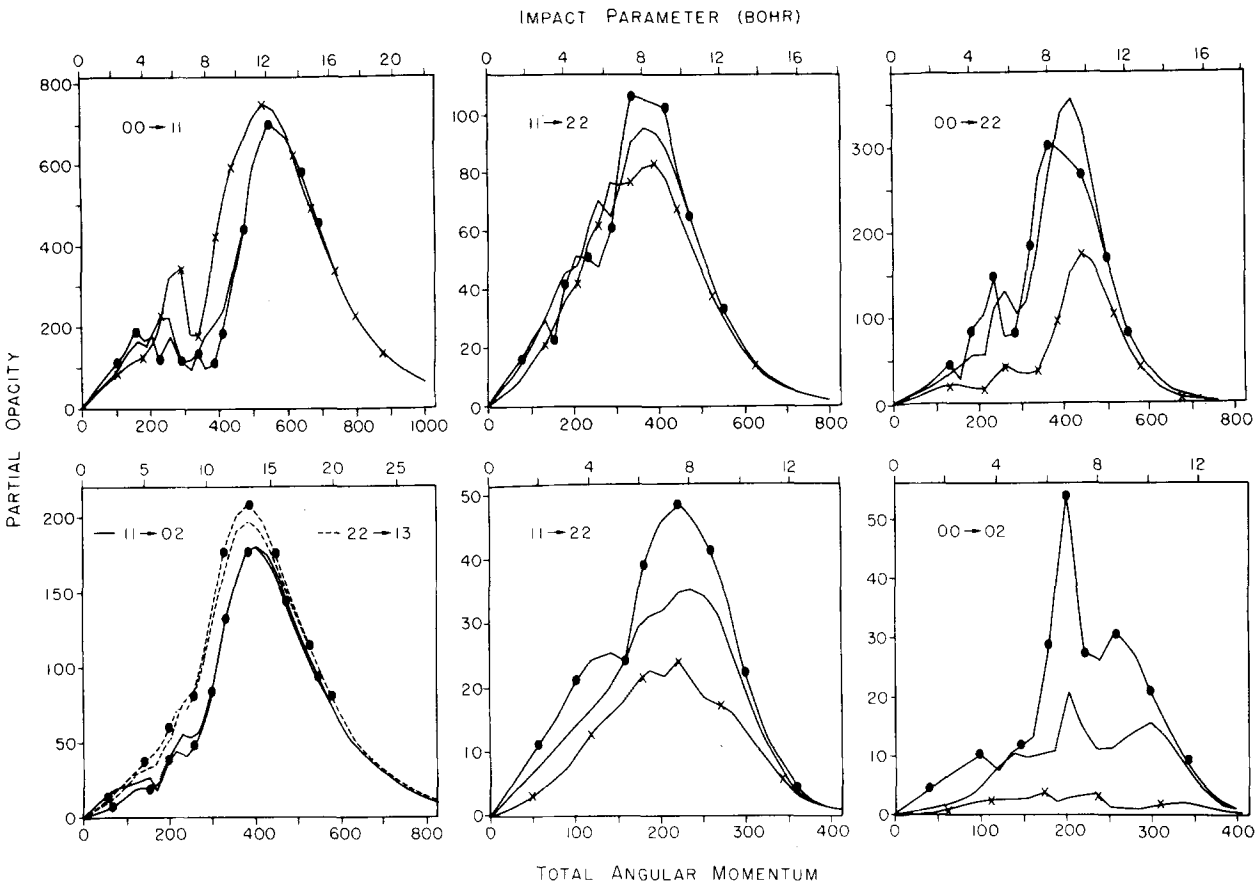

FIG. 1. Representative partial opacities for $E = 12500$ cm^{-1} (top three panels) and $E = 5300$ cm^{-1} (bottom three panels) as a function of the total angular momentum. The corresponding semiclassical impact parameter [Eq. (21)] is also indicated. The displayed traces refer to the B3, B4, and B5 channel bases described in Table II. To aid in visual discrimination the B3 results are labeled with x's and the B5 results, with filled circles. In the lower left panel the continuous traces refer to the 11→02 transition; the dashed traces, to the 22→13 transition. For clarity the B3 11→02 opacities are absent from this panel. For the transitions out of the $j_1 j_2 = 00$ level the displayed opacities correspond to (+) interchange symmetry [Eq. (13)]; it should be remembered that these quantities vanish at every odd value of J. For the transitions not involving the $j_1 j_2 = 00$ level, the interchange averaged opacities [Eq. (18)] are displayed.

reversibility [Eq. (19)].

The dominance of the cross section for the first-order dipole–coupled R–R transitions is obvious, especially at the lower end of the energy range covered here. For the $j_1 j_2 = 11$ initial state between 60% (at $E = 12\,500$ cm^{-1}) and 75% (at $E = 3900$ cm^{-1}) of the inelastic flux proceeds by the 11→02 transition. We remind the reader that these results apply to the simplified potential, which contains only the dipole–dipole anisotropy. As will be seen in the next section, the presence of the other anisotropic components leads to additional inelastic pathways with substantial flux.

Rotationally inelastic cross sections are often compared with gas kinetic cross sections. For the HF–HF system the latter quantity will be $\simeq 27$ Å^2, if we assume that the hard sphere radius of the spherically symmetric component in the present potential (5.5 bohr) provides a good estimate of an effective hard sphere radius for the system, or, alternatively, 19 Å^2 if we use the semiempirical hard sphere radius of Zeleznik and Svehla.[30] In either case it is clear that the dipole–dipole R–R cross sections are several times gas kinetic. This arises, of course, because such large impact parameters contribute to the transition (Fig. 1). In fact even at the peak in the partial opacity curves, the individual transition probabilities are much less than unity.

V. RESULTS: FULL POTENTIAL

As discussed in Sec. III, since the full potential couples states of even and odd rotational parity, $(-1)^{j_1+j_2}$, the number of channels is much larger, so that it was not practical to carry out calculations with a B5 basis. Consequently, we restricted the calculations with the full potential to $E \geq 6000$ cm^{-1}, where, to judge from the results with the simplified potential (Table IV), a reasonable degree of convergence can be obtained with a B4 basis. Integral cross sections are listed in Table VI, and partial opacities for three representative transitions at $E = 9500$ cm^{-1} are displayed in Fig. 2. It is interesting to observe that the cross sections for the strong first-order dipole-coupled transitions (00→11, 11→02, 22→13) are only slightly reduced below the comparable values for the pure dipole–dipole potential (Table IV). For those transitions the major inelasticity occurs at

TABLE VI. Integral cross sections (Å^2); full potential.[a]

Transition	Basis[a]	Total energy (cm^{-1}) 6000	7000	8000	9500	11 000	12 500
Dipole-allowed							
00→ 11	B3	45.0	51.6	57.3	59.9	62.3	62.8
	B4	43.8	49.4	52.6	55.1	54.7	55.5
00→ 02	B3	3.5	4.8	5.8	5.9	6.7	7.1
	B4	4.6	5.9	7.2	7.1	7.5	7.1
00→ 22	B3	1.1	1.5	2.1	3.4	5.3	6.5
	B4	2.1	3.5	5.1	6.9	8.9	10.7
00→ 13	B3[b]	...	...	...	...	...	...
	B4	1.0	1.4	1.8	2.0	2.9	3.3
11→ 02	B3	52.1	53.6	54.1	54.4	52.7	51.1
	B4	52.8	53.6	53.0	52.2	49.6	46.8
11→ 22	B3	3.8	4.8	5.7	6.9	7.9	9.0
	B4	5.4	6.2	6.9	7.8	8.6	9.2
11→ 13	B3[b]	...	...	...	...	...	...
	B4	2.7	3.4	3.9	5.1	6.0	6.9
22→ 13	B3[b]	...	...	...	...	...	...
	B4	62.4	63.9	63.5	64.1	61.5	59.1
01→ 12	B3	27.7	33.7	40.0	47.1	53.7	60.5
	B4	34.2	39.9	43.4	50.8	57.1	56.5
12→ 03	B3[c]	...	...	...	...	...	...
	B4	23.3	28.5	30.6	34.9	37.9	39.5
12→ 23	B3[b]	...	...	...	...	...	...
	B4	8.9	9.3	10.7	11.3	12.4	13.4
Dipole-forbidden[d]							
00→ 01	B3	7.1	7.6	7.4	7.8	7.5	7.8
	B4	7.0	8.5	10.1	8.4	9.4	8.7
00→ 12	B3	1.7	2.0	2.5	3.3	3.8	4.2
	B4	3.1	4.3	4.8	5.1	6.4	7.2
00→ 03	B3	0.2	0.3	0.4	0.6	1.0	0.8
	B4	0.4	0.5	0.6	1.0	1.0	1.1
01→ 11	B3	18.6	18.9	18.9	17.5	15.8	14.7
	B4	18.8	18.5	16.9	15.0	13.5	13.1
01→ 02	B3	6.5	6.7	7.1	7.7	7.8	7.9
	B4	8.7	9.1	9.5	9.8	9.7	9.8
01→ 03	B3	2.2	2.8	3.5	4.8	6.2	7.2
	B4	1.7	2.0	2.3	3.4	3.7	4.6
01→ 22	B3	4.4	5.1	6.3	7.4	7.9	9.5
	B4	7.3	7.7	7.9	8.6	8.3	8.7
11→ 12	B3	8.0	8.6	8.9	9.7	9.7	9.8
	B4	12.0	12.2	11.9	11.8	11.3	10.6
11→ 03	B3	1.1	1.2	1.5	1.6	1.7	1.8
	B4	1.2	1.3	1.4	1.7	1.9	2.0
12→ 22	B3[c]	...	...	...	...	...	...
	B4	16.1	15.4	14.9	14.0	13.3	12.6
12→ 13	B3[b]	...	...	...	...	...	...
	B4	11.7	11.5	12.1	11.9	12.1	12.4
03→ 13	B3[b]	...	...	...	...	...	...
	B4	30.3	28.2	25.8	26.2	23.5	21.6
22→ 03	B3	8.2	7.6	7.2	6.8	6.6	6.2
	B4	4.2	4.1	3.4	3.6	3.2	3.1
22→ 23	B3[b]	...	...	...	...	...	...
	B4	8.4	8.3	8.3	9.4	8.7	8.7

[a]See Table II for description of channel basis.
[b]These transitions are not allowed with a B3 basis.
[c]By oversight the opacities and cross sections for these transitions were not determined with a B3 basis.
[d]The following transitions are not dipole–dipole coupled, to any order, since the initial and final states are of opposite rotational parity, defined as $(-1)^{j_1+j_2}$.

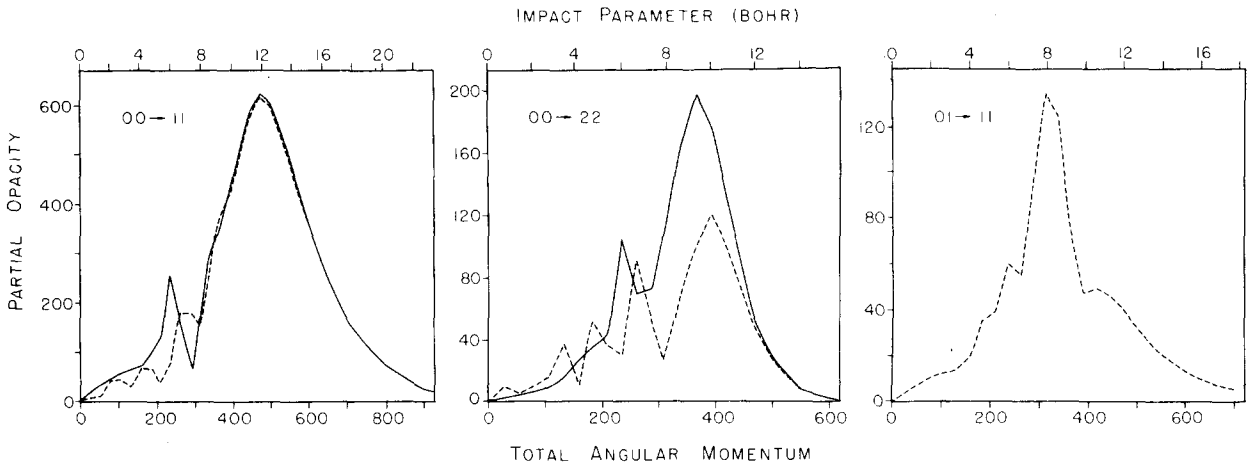

FIG. 2. Representative partial opacities for $E = 9500$ cm^{-1} as a function of the total angular momentum. The corresponding semiclassical impact parameter [Eq. (21)] is also indicated. The continuous traces refer to the simplified (dipole–dipole) potential; the dashed traces, to the full potential. The 01 → 11 transition is dipole–dipole forbidden, therefore, there is no continuous trace in the right-hand panel. A B4 channel basis (Table II) was used for the calculations with both surfaces. For the transitions out of the $j_1 j_2 = 00$ level the displayed opacities correspond to (+) interchange symmetry [Eq. (13)]; it should be remembered that these quantities vanish at every odd value of J. For the transitions not involving the $j_1 j_2 = 00$ level, the interchange averaged opacities [Eq. (18)] are displayed.

large impact parameters where the effect of the additional anisotropic terms is negligibly small. This can be seen clearly in the 00 → 11 opacity curves plotted in Fig. 2.

By contrast, for all the other dipole-allowed transitions the cross sections are substantially reduced below the values obtained with the pure dipole–dipole potential (Table IV). Here the major inelasticity occurs at smaller impact parameters (Figs. 1 and 2) where the additional anisotropic terms are sizeable. Examination of Table IV shows that the flux which has been lost from these transitions reappears in dipole-forbidden transitions, especially those of the type

$$j_1 j_2 \rightarrow j_1, j_2 \pm 1 \tag{21a}$$

or, equivalently,

$$j_1 j_2 \rightarrow j_1 \pm 1, j_2 , \tag{21b}$$

which are directly coupled by the short range A_{011} anisotropic term in the potential. In fact, over the energy range studied here, the cross sections associated with these transitions are as large or larger than those for the second-order dipole-allowed processes. Additionally, the cross sections for transitions of type (21) appear to be reasonably well converged with a B4 basis, in contrast to the observed behavior (Table IV) of the second-order dipole-allowed cross sections. Also, one can see from Fig. 2 that despite the shorter range of the A_{011} anisotropy, the range of impact parameters which contribute substantially to the partial opacities for transitions of type (21) is comparable to what we have observed for the second-order dipole-allowed transitions (Figs. 1 and 2).

Since λ_1 [Eq. (1)] is zero for the A_{011} anisotropy, the coupling matrix elements for transitions (21a) and (21b) will be independent of the rotational quantum number which does not change.[50] To first-order the corresponding cross sections should display the same invariance. This effect is seen in a comparison of the 01 → 02, 11 → 12, and 12 → 22 cross sections or the 12 → 13 and 22 → 23 cross sections. The slight variations in the individual values reflect, of course, the effect of the direct dipole-quadrupole (A_{123}) coupling or higher-order coupling involving the A_{011} and A_{112} terms, all of which will introduce some degree of dependence on the unchanged rotational quantum number.

The cross sections for the transitions which are coupled in first-order by just the dipole–quadrupole interaction (00 → 12, 01 → 22, 11 → 03, 22 → 03) are all relatively small. This is particularly surprising for the R–R 22 → 03 transition which is out of resonance by only 0.15 cm^{-1}. Despite this fact, the 22 → 03 cross sections are more than an order of magnitude smaller than the values for the R–R 11 → 02 and 22 → 13 processes which have much larger inelastic energy gaps ($\Delta E = 41$ cm^{-1}) but which are coupled by the dipole–dipole potential. Clearly, the magnitudes of R–R cross sections may be more dependent on the range and magnitude of the various long range anisotropic terms than on the degree of resonance. Study of the 22 → 03 opacity curves (not shown) reveals that large impact parameter collisions really do not contribute to this transition.

In experiments where resolution of the final rotational states is not possible, the physically important quantities are total inelastic cross sections for depopulation of a given initial state. These quantities are defined by

$$\sigma_{j_1 j_2} = \sum_{j_1' j_2'} \sigma_{j_1 j_2 \rightarrow j_1' j_2'} . \tag{22}$$

Table VII compares the total inelastic cross sections for the $j_1 j_2 = 00$ and 11 initial states, obtained from our calculations with both the simplified and full potentials. The values appear to be relatively insensitive to the choice of channel basis or to the inclusion of the addi-

TABLE VII. Total inelastic cross sections (Å^2).[a]

	$j_1 j_2 = 00$			$j_1 j_2 = 11$		
	Dipole–dipole		Full	Dipole–dipole		Full
E (cm^{-1})	B4	B5	B4	B4	B5	B4
6 000	59	61	62	75	78	85
7 000	66	71	74	78	81	88
8 000	72	81	82	80	82	89
9 500	79	89	86	80	83	90
11 000	85	93	91	80	83	88
12 500	88	92	94	80	81	86

[a]Equation (22). The indicated channel bases are described in Table II.

tional anisotropic terms in the potential. As was discussed earlier in this section, the loss of flux into the second-order dipole-allowed transitions is compensated by the appearance of flux in the dipole-forbidden transitions. Also, approximately 60% of the total inelastic flux is concentrated in certain dipole-allowed transitions for which the cross sections are little affected by the additional anisotropic terms.

VI. DISCUSSION

We have presented here the results of a detailed study of rotational energy transfer in the HF–HF system based on complete quantum mechanical solutions of the equations of motion for two fits to the *ab initio* potential surface of Yarkony *et al.*[22] Our major conclusions are as follows:

(1) For collisions between identical polar molecules, it is currently feasible to carry out full close-coupling determinations of cross sections for transitions between the lower rotational levels. The calculations become particularly manageable if just the dipole–dipole anisotropy is retained, which permits a further decoupling of the equations.

(2) The largest cross sections are associated with the dipole-allowed R–R transitions of the type $j_1 j_2 \rightarrow j_1 \pm 1$, $j_2 \mp 1$, and with the $00 \rightarrow 11$ $T \rightarrow R$ process. The major contribution to these cross sections arise from collisions at large impact parameter (there to five times the hard sphere radius). Consequently, the magnitudes of these cross sections are little affected by the presence of other shorter-range components in the intermolecular potential.

(3) The cross sections associated with all other dipole-allowed processes, except those mentioned in the preceding paragraph, are considerably smaller. The maximum in the partial opacity curves occur at smaller impact parameter, albeit larger than the HF–HF dimer separation. The magnitudes of the cross sections for these processes are sensibly reduced when shorter-range components are included in the potential.

(4) The cross sections associated with transitions which are dipole-forbidden but allowed by the short-range basically repulsive anisotropic component are, in general, comparable in magnitude to the cross sections discussed in the preceding paragraph. By contrast the transitions which are coupled by only the dipole–quadrupole interaction have small cross sections, even in the case of the $22 \rightarrow 03$ transition which is in nearly exact resonance.

Although the above conclusions are strictly applicable only to the HF–HF system at hyperthermal energies, we feel that these results can shed new light on the general mechanism of rotational energy transfer between polar molecule. An obvious comment concerns the role of long range multipole forces. It is clear that the strong R–R transitions, which are responsible for the major portion of the total inelastic cross sections, can be attributed solely to the dipole–dipole interaction. However, the many other transitions appear to be sensitive to both the dipole–dipole term and the shorter-range anisotropic components. Additionally, basically repulsive interactions may in many cases be more important than the higher order multipole terms (dipole–quadrupole, quadrupole–quadrupole). Consequently, theoretical models based solely on the long-range multipole expansion of the interaction potential[12,13,16,17,51,52] will become increasingly inadequate as improvements in experimental technique allow a finer degree of initial and final state resolution.

For many bimolecular systems close-coupling calculations will be too difficult and too expensive, particularly in the case of nonidentical collision partners. It is important, especially in view of the recent experimental advances,[4–11] to continue the development of reasonably accurate, computationally faster models which can be used to gain theoretical insight into the mechanism of rotational energy transfer in a wide variety of polar systems. To date, the paucity of accurate cross sections and the degree of rotational state averaging associated with available experimental data have made it difficult to evaluate critically the many approximation techniques which have been developed. The present set of cross sections will provide a far more exacting set of standards.

Unfortunately, a detailed comparison of the CC cross sections given here with the predictions of various approximation techniques[13,16,17,20,21,27,48,51–53] is beyond the scope of the present article. In this context, however, it is worthwhile to point out that our previously published[15] cross sections at $E = 8000$ cm^{-1} obtained using the decoupled l-cominant approximation[54] agree far better with the converged B5 CC values in Table IV than with the unconverged B3 values, which was the only possible comparison at the time of our earlier study. Also, the dipole–dipole cross sections (Table IV) have already been used[43] to examine the adequacy of energy gap parametrizations[44–46] of degeneracy averaged rotationally inelastic cross sections for polar molecule collisions.

One final observation: Table VII indicates that the total inelastic cross sections do not change dramatically when shorter-range anisotropic terms are included in the intermolecular potential. Consequently, if one is only interested in these quantities it may be reasonable to retain only the dipole–dipole term. As we have discussed, the calculations are substantially easier, due to the additional decoupling between states of different ro-

tational parity. An obvious corollary is that experiments which measure only total inelastic cross sections are probably sensitive mainly to the dipole–dipole interaction and do not provide a fine probe of the short-range behavior of the potential.

ACKNOWLEDGMENTS

This work was supported in part by the National Science Foundation, Grant CHE78-08729; by the U.S. Army Research Office, grant DAAG29-78-G-1110; by the Computer Science Center and General Research Board, University of Maryland; and by the National Resource for Computation in Chemistry under a grant from the National Science Foundation and the Basic Energy Sciences Division of the United States Department of Energy under Contract No. W-7405-ENG-48.

The author is grateful to Paul Dagdigian and Andrew DePristo for their encouragement during the course of this study and for helpful comments on the manuscript. He would also like to thank Dale Spangler and Lowell Thomas of the NRCC staff for their help in implementing the calculations at LBL.

[1]G. Birnbaum, Adv. Chem. Phys. **12**, 487 (1967).
[2]R. G. Gordon, W. Klemperer, and J. I. Steinfeld, Ann. Rev. Phys. Chem. **19**, 215 (1968).
[3]C. G. Gray and J. Van Kranendonk, Can. J. Phys. **44**, 2411 (1966).
[4]U. Borkenhagen, H. Malthan, and J. P. Toennies, Chem. Phys. Lett. **41**, 222 (1976); J. Chem. Phys. **71**, 1722 (1979).
[5]A. M. G. Ding and J. C. Polanyi, Chem. Phys. **10**, 39 (1975).
[6]B. A. Esche, R. E. Kutina, N. C. Lang, J. C. Polanyi, and R. M. Rulis, Chem. Phys. **41**, 183 (1979).
[7]J. J. Hinchen and R. H. Hobbs, J. Chem. Phys. **65**, 2732 (1976); J. Appl. Phys. **50**, 628 (1979).
[8]P. J. Dagdigian, B. E. Wilcomb, and M. H. Alexander, J. Chem. Phys. **71**, 1670 (1979).
[9]P. J. Dagdigian and M. H. Alexander, J. Chem. Phys. **72**, 6513 (1980).
[10]J. R. Williams and S. G. Kukolich, Chem. Phys. **36**, 201 (1979).
[11]J. K. Lampert, G. M. Jursich, and F. F. Crim, Chem. Phys. Lett. **71**, 258 (1980); F. F. Crim, private communication (1980).
[12]R. J. Cross, Jr. and R. G. Gordon, J. Chem. Phys. **45**, 3571 (1966).
[13]H. A. Rabitz and R. G. Gordon, J. Chem. Phys. **53**, 1815, 1831 (1970); M. R. Verter and H. Rabitz, *ibid.* **59**, 3816 (1973).
[14]For an excellent review, see G. G. Balint–Kurti, in *Theoretical Chemistry*, MTP International Review of Science, Physical Chemistry, Series 2 (Butterworths, London, 1975), Vol. 1.
[15]A. E. DePristo and M. H. Alexander, J. Chem. Phys. **66**, 1334 (1977).
[16]M. H. Alexander and A. E. DePristo, J. Phys. Chem. **83**, 1999 (1979).
[17]M. H. Alexander, J. Chem. Phys. **71**, 6183 (1979).
[18]R. Bernstein and K. H. Kramer, J. Chem. Phys. **40**, 200 (1964).
[19]R. J. Cross, Jr., J. Chem. Phys. **55**, 510 (1971).
[20]J. C. Polanyi and N. Sathyamurthy, J. Phys. Chem. **83**, 978 (1979).
[21]A. F. Turfa and R. A. Marcus, J. Chem. Phys. **70**, 3035 (1979).
[22]D. R. Yarkony, S. V. O'Neill, H. F. Schaefer III, C. P. Baskin, and C. F. Bender, J. Chem. Phys. **60**, 855 (1974).
[23]M. L. Klein, I. R. McDonald, and S. F. O'Shea, J. Chem. Phys. **69**, 63 (1978).
[24]W. L. Jorgensen, J. Chem. Phys. **70**, 5888 (1979).
[25]M. H. Alexander and A. E. DePristo, J. Chem. Phys. **65**, 5009 (1976).
[26]An alternate fit to the surface of Yarkony *et al.* (Ref. 22) has been reported subsequently [L. L. Poulsen, G. D. Billing, and J. I. Steinfeld, J. Chem. Phys. **68**, 5121 (1978)]. Unfortunately, the functional form chosen is inappropriate for a quantum scattering calculation.
[27]J. S. Alper, M. A. Carroll, and A. Gelb, Chem. Phys. **32**, 471 (1978).
[28]G. Zarur and H. Rabitz, J. Chem. Phys. **60**, 2057 (1974).
[29]S. Green, J. Chem. Phys. **62**, 2271 (1975).
[30]It should be pointed out that these parameters differ considerably from the values ($\sigma = 4.7$ bohr, $\epsilon = 0.03$ eV) obtained from viscosity data [F. J. Zeleznik and R. A. Svehla, J. Chem. Phys. **53**, 632 (1970)].
[31]T. R. Dyke, B. J. Howard, and W. Klemperer, J. Chem. Phys. **56**, 2442 (1972).
[32]D. F. Smith, J. Mol. Spectrosc. **3**, 473 (1959); E. U. Frank and F. Meyer, Z. Electrochem. **63**, 577 (1959).
[33]A more detailed comparison of the avialable *ab initio* predictions is given in Ref. 25.
[34]H. Rabitz, "Effective Hamiltonians in Molecular Collisions," in *Modern Theoretical Chemistry*, edited by W. H. Miller (Plenum, New York, 1976), Vol. 2.
[35]M. H. Alexander and A. E. DePristo, J. Chem. Phys. **66**, 2166 (1976).
[36]R. G. Gordon, J. Chem. Phys. **51**, 14 (1969); Meth. Comput. Phys. **10**, 81 (1971).
[37]M. H. Alexander, Proceedings, NRCC Workshop on Algorithms and Computer Codes for Atomic and Molecular Scattering Theory, edited by L. D. Thomas, 1979, Vol. 1, p. 75. Available as document LBL-9501, UC-4, CONF-790696 from National Technical Information Service, U. S. Department of Commerce, 5285 Port Royal Rd., Springfield VA 22161, price code: A18.
[38]Program 187, Quantum Chemistry Program Exchange, Indiana University, Bloomington, IN 61701.
[39]Proceedings, NRCC Workshop on Algorithms and Computer Codes for Atomic and Molecular Scattering Theory, edited by L. D. Thomas, 1979, Vol. 2 (in press); L. D. Thomas, M. H. Alexander, B. R. Johnson, W. A. Lester, Jr., J. C. Light, K. D. McLenithen, G. A. Parker, M. J. Redmon, T. G. Schmalz, D. Secrest, and R. B. Walker, J. Comput. Phys. (to be published).
[40]For further discussions of the relations between symmetrized and unsymmetrized cross sections see Refs. 28 and 29 and W. D. Davison, Discuss. Faraday, Soc. **33**, 71 (1962).
[41]A. E. DePristo and H. Rabitz, J. Chem. Phys. **72**, 4685 (1980).
[42]The classical dynamical threshold is defined as the collision energy above which the particular initial and final states will be joined by at least one real valued classical trajectory. [J. Stine and R. A. Marcus, Chem. Phys. Lett. **15**, 536 (1972); S. D. Augustin and W. H. Miller, *ibid.* **28**, 149 (1974).] It is generally thought that the classical dynamical threshold will coincide roughly with the first maximum in the energy dependence of the inelastic cross section. See, for example, S. C. Cohen and M. H. Alexander, J. Chem. Phys. **61**, 3967 (1974).
[43]M. H. Alexander, E. F. Jendrek, and P. J. Dandigian, J. Chem. Phys. **73**, 3797 (1980).
[44]J. C. Polanyi and K. B. Woodall, J. Chem. Phys. **56**, 1563 (1972).
[45]R. D. Levine, R. B. Bernstein, P. Kahana, I. Procaccia, and E. T. Upchurch, J. Chem. Phys. **64**, 796 (1976); R. D. Levine, Ann. Rev. Phys. Chem. **29**, 59 (1978).
[46]D. E. Pritchard, N. Smith, R. D. Driver, and T. A. Brunner, J. Chem. Phys. **70**, 2115 (1979).

[47]M. H. Alexander, J. Chem. Phys. **71**, 5212 (1979).
[48]R. Goldflam and D. J. Kouri, J. Chem. Phys. **70**, 5076 (1979).
[49]A. E. DePristo, S. D. Augustin, R. Ramaswamy, and H. Rabitz, J. Chem. Phys. **71**, 850 (1979).
[50]The potential matrix elements (Refs. 15 and 29) contain the product of several angular momentum coupling coefficients. In the case where $\lambda_1 = 0$, several of these coefficients can be simplified and reduced, and all dependence on j_1 eliminated. A similar reduction involving j_2 occurs if $\lambda_2 = 0$.
[51]L. Biolsi, J. Chem. Phys. **65**, 2541 (1976).
[52]S. C. Mehrotra and J. E. Boggs, J. Chem. Phys. **62**, 1453 (1975).
[53]S. S. Battacharyya and S. Saha, J. Chem. Phys. **68**, 4292 (1978).
[54]A. E. DePristo and M. H. Alexander, J. Chem. Phys. **64**, 3009 (1976).